Mechanisms of Functional Mitral Regurgitation in Ischemic Cardiomyopathy Determined by Transesophageal Echocardiography (from the Surgical Treatment for Ischemic Heart Failure Trial)

Krzysztof Golba, MD[a], Krzysztof Mokrzycki, MD, PhD[b], Jaroslaw Drozdz, MD[c], Alexander Cherniavsky, MD[d], Krzysztof Wrobel, MD[e], Bradley J. Roberts, MD[f], Haissam Haddad, MD[g], Gerald Maurer, MD[h], Michael Yii, MB, MS[i], Federico M. Asch, MD[j], Mark D. Handschumacher, BS[k], Thomas A. Holly, MD[l], Roman Przybylski, MD[m], Irving Kron, MD[n], Hartzell Schaff, MD[o], Susan Aston, RN[f], John Horton, MS[p], Kerry L. Lee, PhD[p,q], Eric J. Velazquez, MD[p,r], and Paul A. Grayburn, MD[f,*], for the STICH TEE Substudy Investigators

The mechanisms underlying functional mitral regurgitation (MR) and the relation between mechanism and severity of MR have not been evaluated in a large, multicenter, randomized controlled trial. Transesophageal echocardiography (TEE) was performed in 215 patients at 17 centers in the Surgical Treatment for Ischemic Heart Failure (STICH) trial. Both 2-dimensional (n = 215) and 3-dimensional (n = 81) TEEs were used to assess multiple quantitative measurements of the mechanism and severity of MR. By 2-dimensional TEE, leaflet tenting area, anterior and posterior leaflet angles, mitral annulus diameter, left ventricular (LV) end-systolic volume index, LV ejection fraction (LVEF), and sphericity index ($p < 0.05$ for all) were significantly different across MR grades. By 3-dimensional TEE, mitral annulus area, leaflet tenting area, LV end-systolic volume index, LVEF, and sphericity index ($p < 0.05$ for all) were significantly different across MR grades. A multivariate analysis showed a trend for annulus area ($p = 0.069$) and LV end-systolic volume index ($p = 0.071$) to predict effective regurgitant orifice area and for annulus area ($p = 0.018$) and LV end-systolic volume index ($p = 0.073$) to predict vena contracta area. In the STICH trial, multiple quantitative parameters of the mechanism of functional MR are related to MR severity. The mechanism of functional MR in ischemic cardiomyopathy is heterogenous, but no single variable stands out as a strong predictor of quantitative severity of MR. **(Am J Cardiol 2013;112:1812−1818)**

Functional mitral regurgitation (MR) is a common complication of ischemic heart disease, which is associated with increased mortality.[1−5] Early studies of the mechanism of functional MR focused on mitral annular dilation and loss of systolic annular contraction due to left ventricular (LV) dilation,[6] diminished mitral leaflet closing force,[7] and abnormal LV shape.[8] More recently, it has been shown that functional MR is caused by leaflet tethering as the papillary muscles are displaced apically and laterally by LV dilation.[9−13] Papillary muscle displacement may be due to global or regional wall motion abnormalities and may be symmetric or asymmetric.[14] Understanding the mechanisms of functional MR in any given patient has important implications regarding the correct approach to repair it. To date, neither large prospective studies have examined the mechanism(s) underlying functional MR in ischemic cardiomyopathy nor has the relation between mechanism and severity of functional MR been determined. This is a report of a prospectively defined ancillary study to the Surgical Treatment for Ischemic Heart Failure (STICH) trial, in which 2-dimensional (2D) and 3-dimensional (3D) transesophageal echocardiographies (TEE) were used to define the mechanism(s) of functional MR in a large clinical trial of patients with ischemic cardiomyopathy randomized to medical therapy, coronary bypass grafting, or coronary bypass grafting plus surgical ventricular restoration.[15,16]

Methods

All participating STICH study sites were invited to participate in the STICH MR TEE substudy; 17 accepted.

[a]Medical University of Silesia, Katowice, Poland; [b]Klinika Kardiochirurgii, PUM, Szczecin, Poland; [c]Medical University of Lodz, Lodz, Poland; [d]Research Institute of Circulation Pathology, Novosibirsk, Russia; [e]John Paul II Hospital, Krakow, Poland; [f]Baylor University Medical Center, Dallas, Texas; [g]University of Ottawa Heart Institute, Ottawa, Ontario, Canada; [h]Medical University of Vienna, Vienna, Austria; [i]Department of Surgery, St. Vincent's Hospital-Melbourne, University of Melbourne, Melbourne, Australia; [j]MedStar Washington Hospital Center, Washington, DC; [k]Massachusetts General Hospital, Harvard Medical School, Boston, Massachusetts; [l]Northwestern University Feinberg School of Medicine, Chicago, Illinois; [m]Silesian Center for Heart Diseases, Silesian Medical University, Zabrze, Poland; [n]University of Virginia Health System, Charlottesville, Virginia; [o]Mayo Clinic College of Medicine, Rochester, Massachusetts; and [p]Duke Clinical Research Institute, [q]Department of Biostatistics and Bioinformatics, and [r]Division of Cardiology, Department of Medicine, Duke University School of Medicine, Durham, North Carolina. Manuscript received July 15, 2013; revised manuscript received and accepted July 24, 2013.

This work was supported by grants RO1HL72430, UO1HL69015, and UO1HL60913 from the National Institutes of Health, Bethesda, Maryland.

See page 1817 for disclosure information.

*Corresponding author: Tel: (214) 820-7500; fax: (214) 820-7533.

E-mail address: paulgr@baylorhealth.edu (P.A. Grayburn).

0002-9149/13/$ - see front matter
http://dx.doi.org/10.1016/j.amjcard.2013.07.047

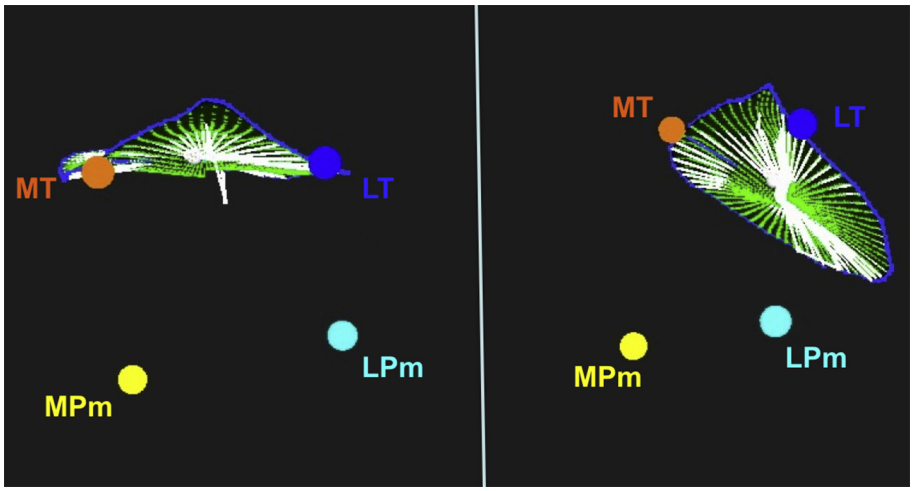

Figure 1. Three-dimensional reconstruction of TEE images using the Omni 4D software. *Blue line* represents mitral annulus and *green and white lines* represent the leaflet area. The medial fibrous trigone *(MT, orange dot)*, lateral fibrous trigone *(LT, dark blue dot)*, medial papillary muscle *(MPm, yellow dot)*, and lateral papillary muscle *(LPm, light blue dot)* are shown.

All 17 sites were provided with a detailed study protocol for obtaining TEE images to define the mechanism and severity of functional MR.[17–19] An Institutional Review Board approval was obtained from each site, and written informed consent was obtained from all patients. At the time the STICH trial was initiated, real-time 3D imaging was not available. Sites equipped with a Philips ultrasound machine (Philips Ultrasound, Andover, Massachusetts) were capable of 3D TEE acquisitions using a rotational reconstruction algorithm.[20] Philips graciously provided the 3D software to those sites. For patients in STICH trial randomized to medical therapy, TEE was done within 1 week of randomization. For patients randomized to surgery, a baseline preoperative TEE was done within 1 week before surgery. Intraoperative TEE was excluded by the study protocol because general anesthesia dramatically reduces the severity of MR by TEE.[21]

TEE was performed during intravenous conscious sedation and local oropharyngeal anesthesia. Heart rate, blood pressure, oxygen saturation, and electrocardiogram were monitored throughout the procedure. Transgastric short-axis views of the LV were obtained at the midpapillary muscle and mitral leaflet levels. A transgastric long-axis view was also oriented to show both papillary muscles with their chordal attachments to the mitral leaflets. From the mid-esophagus, the probe was retroflexed to obtain a 4-chamber view with care to maximize LV cavity length and width while keeping the LV long axis in the center of the imaging sector. From this position, the imaging plane was manually rotated to obtain a commissural view, a 2-chamber view, and a long-axis view. For sites with 3D capability, at least two 3D rotational scans were obtained in each patient. Translational artifacts secondary to patient respiration were minimized using a proprietary software to automatically capture images within a defined respiratory threshold. After obtaining a well-aligned 4-chamber view, the probe was rotated automatically in 6° increments by the 3D TEE software across a total of 180°. These images were downloaded onto a 5.25″ magneto-optic disk and sent to the core laboratory, where analysis was performed in a blinded fashion using a custom software (Omni 4D; Massachusetts General Hospital, Boston, Massachusetts). This offered several advantages with regard to quality control. First, this software has been previously validated in vitro and in vivo.[10–13] Second, it allowed the different TEE operators at different STICH sites to get consistent high-quality data from a single midesophageal probe position during quiet respiration or breath hold. Third, it allowed more accurate measurements without confounding by foreshortened or off-axis views or flattening of 3D measurements onto a 2D display screen.

The mechanism(s) of functional MR was assessed by quantitative measurements including leaflet tethering distance, tethering angle, tenting area, papillary muscle displacement, and annulus area at end-diastole and end-systole. Three-dimensional TEE data sets were analyzed using the method by Otsuji et al.[11] Manual tracing was used to identify the hinge points of the mitral leaflet insertion to identify the mitral annulus in each rotational imaging plane. The aortic annulus was identified by the hinge points of aortic leaflet insertion, and the intersection of the aortic and mitral annuli allowed identification of the medial and lateral fibrous trigones. The tips of the papillary muscles were also identified. In cases with complex papillary muscle anatomy, the largest papillary muscle head, which was most centrally located, was selected. All these points were assigned different colors by the Omni 4D software so that they could be tracked in 3D (Figure 1). The computer allowed rotation of the images to facilitate analysis. The software then automatically calculated the mitral annulus areas at end-diastole and end-systole, the percent systolic contraction of the mitral annulus, the papillary muscle separation distance, the mitral tenting area and height, the papillary muscle separation angle (angle from the posteromedial papillary muscle to the medial trigone to the anterolateral papillary muscle), and the distances between the medial trigone and the posteromedial and anterolateral papillary muscles.

Table 1
Baseline demographic and clinical characteristics: comparison of patients in MR substudy versus not in MR substudy

Variable	STICH H1/H2 Population		p Value
	MR Substudy (n = 214)	Not in MR Substudy (n = 1,922)	
Age (yrs)	60.4 (52.7, 68.0)	60.5 (54.0, 68.1)	0.317
Men	188/214 (87.9)	1,662/1,922 (86.5)	0.574
Women	26/214 (12.1)	260/1,922 (13.5)	
White	195/214 (91.1)	1,473/1,922 (76.6)	<0.001
Black	5/214 (2.3)	45/1,922 (2.3)	
Asian	5/214 (2.3)	235/1,922 (12.2)	
Other	9/214 (4.2)	164/1,922 (8.5)	
Multiracial		5/1,922 (0.3)	
Body mass index (kg/m^2)	27.0 (24.5, 29.4)	26.9 (24.2, 30.1)	0.856
Previous myocardial infarction	183/214 (85.5)	1,559/1,922 (81.1)	0.115
History of hyperlipidemia	147/214 (68.7)	1,245/1,918 (64.9)	0.271
History of hypertension	129/214 (60.3)	1,147/1,922 (59.7)	0.865
Diabetes mellitus	70/214 (32.7)	729/1,922 (37.9)	0.134
Current smoker	39/214 (18.2)	406/1,921 (21.1)	0.320
Previous percutaneous coronary intervention	38/214 (17.8)	294/1,922 (15.3)	0.346
Chronic renal insufficiency	8/214 (3.7)	164/1,920 (8.5)	0.014
Stroke	18/214 (8.4)	123/1,922 (6.4)	0.261
Previous coronary bypass	2/214 (0.9)	58/1,922 (3.0)	0.080
Current Canadian Cardiovascular Society angina class	1.0 (0.0, 3.0)	2.0 (0.0, 3.0)	0.047
None	80/214 (37.4)	586/1,922 (30.5)	0.006
I	29/214 (13.6)	216/1,922 (11.2)	
II	51/214 (23.8)	629/1,922 (32.7)	
III	51/214 (23.8)	400/1,922 (20.8)	
IV	3/214 (1.4)	91/1,922 (4.7)	
Current NYHA heart failure class	2.0 (2.0, 3.0)	2.0 (2.0, 3.0)	<0.001
I	43/214 (20.1)	174/1,922 (9.1)	<0.001
II	111/214 (51.9)	903/1,922 (47.0)	
III	54/214 (25.2)	765/1,922 (39.8)	
IV	6/214 (2.8)	80/1,922 (4.2)	
Systolic blood pressure (mm Hg)	120.0 (110.0, 130.0)	120.0 (110.0, 130.0)	0.123
Diastolic blood pressure (mm Hg)	80.0 (70.0, 80.0)	75.0 (69.0, 80.0)	0.016
Heart rate (beats/min)	72.0 (66.0, 80.0)	72.0 (65.0, 80.0)	0.433
Creatinine (mg/dl)	1.1 (0.9, 1.2)	1.1 (0.9, 1.3)	0.067
Baseline LVEF (%) CMR/RN/echo/site	26.1 (20.2, 32.0)	27.4 (22.0, 33.7)	0.056
End-systolic volume index (ml/m^2)	82.5 (65.0, 103.2)	77.9 (59.6, 98.6)	0.018
Anterior akinesia or dyskinesia (%)	47.0 (29.0, 57.0)	43.0 (35.0, 60.0)	0.382
MR severity grade*			
None or trace	66/212 (31.1)	702/1,912 (36.7)	<0.001
Mild	87/212 (41.0)	886/1,912 (46.3)	
Moderate or severe	59/212 (27.8)	324/1,912 (16.9)	
Baseline medications			
β blocker	195/214 (91.1)	1,631/1,922 (84.9)	0.014
ACE inhibitor or ARB	193/214 (90.2)	1,698/1,922 (88.3)	0.423
ACE inhibitor	187/214 (87.4)	1,550/1,922 (80.6)	0.016
Digoxin	33/214 (15.4)	351/1,922 (18.3)	0.304
Diuretic (potassium sparing)	137/214 (64.0)	752/1,922 (39.1)	<0.001
Diuretic (loop/thiazide or potassium sparing)	169/214 (79.0)	1,360/1,922 (70.8)	0.012
Aspirin (daily)	190/214 (88.8)	1,521/1,922 (79.1)	<0.001
Aspirin or warfarin	197/214 (92.1)	1,625/1,922 (84.5)	0.003
Statin	195/214 (91.1)	1,491/1,922 (77.6)	<0.001

Median (twenty-fifth, seventy-fifth percentiles) for continuous variables and sample/total number (percentage) for categorical variables.
CMR = cine magnetic resonance; RN = radionuclide.
* MR grade by transthoracic echocardiography as determined by study site investigators.

In addition to the mechanistic variables measured from TEE images, core laboratory evaluations of LV end-diastolic volume index and end-systolic volume index, LV ejection fraction (LVEF), and sphericity index were available from the STICH trial database. In the main STICH trial, all patients underwent baseline echocardiography, whereas magnetic resonance imaging and radionuclide imaging were optional. Using methods described previously, optimal LV volumes and LVEF were determined using an approach that incorporated all methods with the best correlation to overall mortality.[22]

Quantitative measurements of MR severity, effective regurgitant orifice area (EROA), and vena contracta width

Table 2
Two-dimensional transesophageal echocardiographic (TEE) measurements of mitral regurgitation (MR) mechanism according to mitral regurgitation grade

Variable	None or Trace (n = 57)	Mild (n = 120)	Moderate or Severe (n = 33)	p Value
Leaflet tenting area (cm^2)	1.5 (1.2, 1.8)	1.6 (1.4, 2.0)	2.1 (1.4, 2.2)	0.080
Leaflet tenting height (cm)	0.7 (0.6, 0.8)	0.8 (0.7, 0.9)	0.8 (0.7, 1.0)	0.611
Anterior leaflet angle (degrees)	40.0 (29.0, 44.0)	38.0 (32.0, 45.0)	38.0 (29.0, 46.0)	0.005
Midanterior leaflet angle (degrees)	148.0 (142.0, 158.0)	149.0 (140.0, 158.0)	147.0 (137.0, 158.0)	0.122
Posterior leaflet angle (degrees)	55.0 (46.0, 65.0)	54.0 (44.0, 64.0)	54.0 (45.0, 69.0)	0.028
Annulus diameter 4-chamber view (cm)	3.4 (3.3, 3.5)	3.4 (3.1, 3.6)	3.5 (3.2, 3.8)	0.654
Annulus diameter long-axis view (cm)	3.2 (2.9, 3.4)	3.3 (3.0, 3.5)	3.5 (3.4, 3.7)	0.004
LV end-systolic volume index (ml/m^2)	77.0 (57.3, 99.6)	81.0 (66.3, 100.2)	99.9 (82.6, 128.9)	<0.001
Baseline LVEF (%)	27.0 (21.8, 33.1)	27.8 (20.0, 32.0)	22.7 (18.8, 26.0)	0.017
Sphericity index	1.4 (1.4, 1.6)	1.4 (1.3, 1.6)	1.3 (1.2, 1.4)	0.008

Median (twenty-fifth, seventy-fifth percentiles) for continuous variables.

Table 3
Three-dimensional transesophageal echocardiographic (TEE) measurements of mitral regurgitation (MR) mechanism according to mitral regurgitation grade

Variable	None or Trace (n = 26)	Mild (n = 44)	Moderate or Severe (n = 11)	p Value
Annulus area diastole (cm^2)	9.8 (9.0, 11.7)	11.8 (10.2, 13.0)	12.0 (11.4, 12.1)	0.002
Annulus area systole (cm^2)	10.1 (9.1, 11.4)	11.5 (10.2, 12.6)	12.2 (11.5, 13.3)	0.001
Annular contraction (%)	−2.3 (−7.9, 0.7)	1.9 (−2.8, 6.8)	−4.9 (−7.4, −3.6)	0.600
Leaflet tenting area (cm^2)	1.6 (1.3, 2.0)	1.9 (1.6, 2.4)	2.4 (2.2, 2.9)	<0.001
Medial trigone to medial papillary muscle distance (mm)	42.5 (41.0, 47.0)	44.6 (40.7, 48.0)	45.1 (43.5, 47.0)	0.295
Lateral trigone to lateral papillary muscle distance (mm)	25.1 (21.7, 29.6)	26.8 (23.3, 30.8)	29.9 (24.9, 34.4)	0.092
Primary chordal separation angle (degrees)	35.4 (28.2, 43.4)	37.3 (30.9, 41.3)	38.9 (33.6, 44.8)	0.082
LV end-systolic volume index (ml/m^2)	80.8 (59.9, 101.7)	88.1 (68.8, 108.3)	114.3 (93.8, 138.1)	0.006
Baseline LVEF (%)	28.5 (21.9, 33.0)	27.0 (21.1, 31.3)	24.2 (18.7, 25.7)	0.050
Sphericity index	1.5 (1.4, 1.5)	1.4 (1.2, 1.6)	1.4 (1.2, 1.5)	0.017

Median (twenty-fifth, seventy-fifth percentiles) for continuous variables.

(VCW) were used. MR was considered to be absent if no color flow signal was detectable superior to the mitral coaptation line during systole by color flow mapping. Trace MR was considered to be present when a few color pixels were present but no defined jet morphology was observed. For purposes of data analysis, none and trace MRs were grouped together. If a defined systolic color flow jet was present, the severity of MR was classified using a hierarchical approach. Accordingly, EROA by the proximal isovelocity surface area method was used to classify MR severity, unless it was of poor technical quality or could not be measured. If no MR was present, EROA was assigned a value of zero. As per the guidelines of the American Society of Echocardiography[23] and the European Association of Echocardiography,[24] mild MR was considered to be an EROA of $\leq$0.2 cm^2, moderate MR 0.2 to 0.39 cm^2, and severe MR $\geq$ 0.4 cm^2. If EROA was not available or measureable, VCW was next used to classify MR severity with <0.3 cm being mild MR and $\geq$0.7 cm being severe MR. If neither EROA nor VCW were available, regurgitant volume by quantitative Doppler was used. If no quantitative measurements were available, the size of the color flow jet was used with $\leq$4.0 cm^2 denoting mild MR, and $\geq$8.0 cm^2 severe MR. Jet eccentricity, E-wave velocity, and pulmonary vein pattern were used to adjust the MR severity up or down by 1 grade using the integrative method described by the American Society of Echocardiography and the European Association of Echocardiography guidelines.[23,24] All patients graded as moderate or severe MR had quantitative assessment of EROA.

Quantitative measurements of annulus size and leaflet tethering were compared in 3 groups of patients—those without MR, with mild MR (EROA <0.2 cm^2), and with at least moderate MR (EROA $\geq$0.2 cm^2). Specific measurements of MR mechanism were compared across MR grades. Analysis of variance was used to compare continuous variables of MR mechanism among the 3 groups of MR severity. Multivariate regression analysis was performed to evaluate which measurements of the mechanism of MR are independent predictors of MR severity as defined by (1) EROA and (2) VCW. For purposes of the multivariate analysis, EROA and VCW were assigned a value of 0 if MR was graded as none or trace.

Results

TEE studies were obtained in 214 subjects; of whom, 81 had both 2D and 3D TEEs performed and 134 had only 2D TEE. Of these, 210 studies (97.7%) were of sufficient quality to assess MR severity. There were 57 patients with no MR, 120 with mild, 29 with moderate, and 4 with severe MR. Of the subset of patients with 3D TEE, 26 had no MR, 44 had mild MR, and 11 had moderate or severe MR. Given the small sample of severe MR and the fact that even moderate MR portends a poor prognosis in heart failure, the moderate and severe MR grades were combined for statistical analysis.

Table 1 lists the demographic and clinical characteristics of the patients in the MR substudy compared with the

Table 4
Univariate analysis of the correlation between mechanism and quantitative severity of MR

Independent Variable	Dependent Variable	DF	p Value
EROA by proximal isovelocity surface area method (cm^2)	Annulus area diastole (cm^2)	56	0.006
	Annulus area systole (cm^2)	55	0.007
	Annular contraction (%)	55	0.674
	3D: leaflet tenting area (cm^2)	56	0.015
	Medial trigone to medial papillary muscle distance (mm)	55	0.173
	Lateral trigone to lateral papillary muscle distance (mm)	55	0.350
	Primary chordal separation angle (degrees)	55	0.775
	LVESVI (ml)	114	0.043
	Baseline LVEF (%)	114	0.157
	Sphericity index	72	0.050
VCW (cm)	Annulus area diastole (cm^2)	78	0.002
	Annulus area systole (cm^2)	77	<0.001
	Annular contraction (%)	77	0.917
	3D: leaflet tenting area (cm^2)	77	0.004
	Medial trigone to medial papillary muscle distance (mm)	77	0.075
	Lateral trigone to lateral papillary muscle distance (mm)	77	0.047
	Primary chordal separation angle (degrees)	77	0.312
	LVESVI (ml)	203	0.002
	Baseline LVEF (%)	203	0.061
	Sphericity index	110	0.008

DF = degrees of freedom; LVESVI = left ventricular end-systolic volume index.

STICH main trial population not included in the substudy. In general, patients in the MR substudy were similar to those in the parent trial, being predominantly white men with a median age of 60 years. There was a greater predominance of whites in the substudy compared with the main trial (91.1% vs 76.6%, $p < 0.0001$), more patients without angina (37.4% vs 30.5%, $p = 0.006$), and more patients with New York Heart Association class I heart failure symptoms (20.1% vs 9.1%, $p < 0.0001$). Patients in the MR substudy tended to have higher diastolic blood pressure (median of 80 vs 75 mm Hg, $p = 0.016$) and higher LV end-systolic volume index (median of 82.5 vs 77.9 ml/m^2, $p = 0.018$). MR severity (as graded by the sites) tended to be slightly worse in patients in the MR substudy (moderate or severe MR in 27.8% vs 16.9%, $p < 0.001$). Finally, patients in the MR substudy had slightly greater usage of the following medications: β blockers, angiotensin-converting enzyme inhibitors, diuretics, aspirin, aspirin or warfarin, and statins ($p < 0.05$ for all).

Table 2 lists the MR mechanistic variables by MR severity grades in the patients with 2D TEE studies. Multiple measurements were statistically significantly different across MR severity grades, including leaflet angle, posterior leaflet angle, mitral annulus diameter in the long-axis view (anteroposterior diameter), LV end-systolic volume index, LVEF, and sphericity index ($p < 0.05$ for all).

Table 5
Multivariate analyses of the correlation between mechanism and quantitative severity of MR

Dependent Variable	Variables	T Value	p Value
EROA	Mitral annulus area at end-diastole (cm^2)	1.86	0.069
	LVESVI (ml)	1.84	0.071
VCW	Mitral annulus area at end-systole (cm^2)	2.42	0.018
	LVESVI (ml)	1.82	0.073

LVESVI = left ventricular end-systolic volume index.

The most strongly predictive measurement of MR grade was LV end-systolic volume index (77 ml/m^2 for none or trace MR, 81 ml/m^2 for mild MR, and 99.9 ml/m^2 for moderate or severe MR, $p < 0.001$).

Table 3 lists the results of MR mechanistic variables for the different grades of MR severity by 3D TEE. As with 2D TEE, multiple measurements showed statistically significant differences among MR grades, including end-diastolic and end-systolic mitral annulus areas, leaflet tenting area, LV end-systolic volume index, LVEF, and sphericity index ($p \leq 0.05$ for all). Leaflet tethering distance (lateral trigone to lateral papillary muscle) tended to be longer in moderate or severe MR but was not statistically significant ($p = 0.092$). The strongest association was with leaflet tenting area (1.6 cm^2 for none or trace MR, 1.9 cm^2 for mild MR, and 2.4 cm^2 for moderate or severe MR, $p < 0.001$).

Table 4 lists the results of a univariate analysis of various MR mechanistic variables as predictors of quantitative MR severity by EROA and VCW, as prespecified in the statistical analysis plan of the MR substudy. Statistically significant correlations were present between EROA and end-diastolic and end-systolic mitral annulus area, leaflet tenting area, baseline LV end-systolic volume index, and sphericity index. Statistically significant correlations existed between VCW and end-diastolic and end-systolic mitral annulus area by 3D TEE, leaflet tenting area, tethering distance from lateral trigone to lateral papillary muscle, baseline LV end-systolic volume index, and sphericity index.

Table 5 lists the results of multivariate analysis using the variables that were statistically significant by univariate analysis. A trend was found between EROA and end-diastolic mitral annulus area ($p = 0.069$) and LV end-systolic volume index ($p = 0.071$). However, R-square values were weak, indicating that none of these variables were strong predictors of EROA. For VCW, only end-systolic annulus area was statistically significant ($p = 0.018$), with a trend for LV end-systolic volume index ($p = 0.073$).

Discussion

It has been well accepted that in ischemic cardiomyopathy, functional MR is primarily caused by LV dilation and/or dysfunction, such that coaptation of normal or nearly normal mitral leaflets is prevented by a combination of reduced systolic closing force, leaflet tethering, and mitral annular dilation. This ancillary study of the STICH trial offered the opportunity to systematically assess many of these variables using high-resolution measurements of the mitral leaflets and annulus by TEE. The results showed that

multiple 2D and 3D TEE measurements were associated with MR severity, emphasizing the complex and heterogenous nature of ischemic functional MR.

Multiple mechanistic variables were associated with qualitative MR grade, including anterior and posterior leaflet angles, anteroposterior mitral annulus diameter, LV end-systolic volume index, LVEF, and sphericity index in the subset of patients who had 2D TEE studies. The strongest of these were leaflet tenting area and LV end-systolic volume index, the only 2 variables with p values $\leq$0.001. In a smaller subset of 81 patients with 3D TEE, end-diastolic and end-systolic mitral annulus areas, leaflet tenting area, LV end-systolic volume index, LVEF, and sphericity index were statistically significantly associated with MR grade. The strongest of these were end-systolic mitral annulus area and mitral leaflet tenting area, both with p values $\leq$0.001.

For patients in whom EROA could be assessed quantitatively, significant correlations were found for annulus area, leaflet tenting area, LV end-systolic volume index, and sphericity index on univariate analysis. However, on multivariate analysis, none of these variables were significantly related to EROA, although there was a trend for end-diastolic annulus area and LV end-systolic volume index. Similar findings were present for VCW, in which only end-systolic annulus area was statistically significant and there was a trend for LV end-systolic volume index. This is probably explained by a strong degree of correlation between the mechanistic variables, which is consistent with the prevailing hypothesis that functional MR is a consequence of LV dilation and dysfunction.

Most of our data come from 2D TEE because many participating sites did not have 3D capability. At the time of recruitment into the STICH trial, the 3D rotational imaging used in this study was state of the art. However, current 3D imaging techniques use real-time imaging, which is less prone to translational artifacts and is recommended for evaluation of mitral valve morphology[25] and quantitation of functional MR severity by planimetry of the vena contracta area.[26]

The final analysis was conducted based on the data taken from 3 different sources: 2D TEE, 3D TEE, and assessment of LV size and by 2D transthoracic echocardiography, radionuclide angiography, and cine magnetic resonance. This may raise doubts about the homogeneity of data.

Finally, the STICH inclusion criteria stipulated enrolling patients with heart failure due to ischemic cardiomyopathy, LVEF $\leq$35%, and anterior akinesia. Patients with functional MR due to isolated inferior or posterolateral wall motion abnormalities are not represented. In such patients, leaflet tethering is likely to play a larger role in the mechanism of functional MR.

Disclosures

E.J.V. and P.A.G. report research grants with Abbott Vascular; no other conflicts of interest to report regarding this manuscript.

1. Grigioni F, Enriquez-Sarano M, Zehr KJ, Bailey KR, Tajik AJ. Ischemic mitral regurgitation: long-term outcome and prognostic implications with quantitative Doppler assessment. *Circulation* 2001;103:1759−1764.
2. Grayburn PA, Appleton CP, DeMaria AN, Greenberg BH, Lowes B, Oh J, Plehn J, Rahko P, St John Sutton M, Eichhorn EJ, for the BEST Trial Investigators. Echocardiographic predictors of mortality in patients with advanced heart failure: the BEST Trial. *J Am Coll Cardiol* 2005;45:1064−1071.
3. Trichon BH, Felker GM, Shaw LK, Cabell CH, O'Connor CM. Relation of frequency and severity of mitral regurgitation to survival among patients with left ventricular systolic dysfunction and heart failure. *Am J Cardiol* 2003;91:538−543.
4. Rossi A, Dini FL, Faggiano P, Agricola E, Cicoira M, Frattini S, Simioniuc A, Gullace M, Ghio S, Enriquez-Sarano M, Temporelli PL. Independent prognostic value of functional mitral regurgitation in patients with heart failure. A quantitative analysis of 1256 patients with ischaemic and non-ischaemic cardiomyopathy. *Heart* 2011;97:1675−1680.
5. Deja MA, Grayburn PA, Sun B, Rao V, She L, Krejca M, Jain R, Chua YL, Daly R, Senni M, Mokrzycki K, Menicanti L, Oh JK, Michler M, Wróbel K, Lamy A, Velazquez EJ, Lee KL, Jones RH. Influence of mitral regurgitation on survival in the surgical treatment for ischemic heart failure trial. *Circulation* 2012;125:2639−2648.
6. Boltwood C, Tei C, Wong M, Shah P. Quantitative echocardiography of the mitral complex in dilated cardiomyopathy: the mechanism of functional mitral regurgitation. *Circulation* 1983;68:498−508.
7. Kaul S, Pearlman JD, Touchstone DA, Esquival L. Prevalence and mechanisms of mitral regurgitation in the absence of intrinsic abnormalities of the mitral leaflets. *Am Heart J* 1989;118:763−772.
8. Kono T, Sabbah HN, Rosman H, Alam M, Jafri S, Goldstein S. Left ventricular shape is the primary determinant of functional mitral regurgitation in heart failure. *J Am Coll Cardiol* 1992;20:1594−1598.
9. Levine RA, Schwammenthal E. Ischemic mitral regurgitation on the threshold of a solution from paradoxes to unifying concepts. *Circulation* 2005;112:745−758.
10. He S, Fontaine AA, Schwammenthal E, Yoganathan AP, Levine RA. Integrated mechanism for functional mitral regurgitation: leaflet restriction versus coapting force: in vitro studies. *Circulation* 1997;96:1826−1834.
11. Otsuji Y, Handschumacher MD, Schwammenthal E, Jiang L, Song J, Guerrero JL, Vlahakes GJ, Levine RA. Insights from three-dimensional echocardiography into the mechanism of functional mitral regurgitation: direct in vivo demonstration of altered leaflet tethering geometry. *Circulation* 1997;96:1999−2008.
12. Otsuji Y, Gilon D, Jiang L, He S, Leavitt M, Roy MJ, Birmingham MJ, Levine RA. Restricted diastolic opening of the mitral leaflets in patients with left ventricular dysfunction: evidence for increased valve tethering. *J Am Coll Cardiol* 1998;32:398−404.
13. Hung J, Otsuji Y, Handschumacher MD, Schwammenthal E, Levine RA. Mechanism of dynamic regurgitation orifice area variation in functional mitral regurgitation. *J Am Coll Cardiol* 1999;33:538−545.
14. Kwan J, Shiota T, Agler DA, Popovic ZB, Qin JX, Gillinov MA, Stewart WJ, Cosgrove DM, McCarthy PM, Thomas JD. Geometric differences of the mitral apparatus between ischemic and dilated cardiomyopathy with significant mitral regurgitation. Real-time three-dimensional echocardiography study. *Circulation* 2003;107:1135−1140.
15. Jones RH, Velazquez EJ, Michler RE, Sopko G, Oh JK, O'Connor CM, Hill JA, Menicanti L, Sadowski Z, Desvigne-Nickens P, Rouleau JL, Lee KL, for the STICH Hypothesis 2 Investigators. Coronary bypass surgery with or without surgical ventricular reconstruction. *N Engl J Med* 2009;360:1705−1717.
16. Velazquez EJ, Lee KL, Deja MA, Jain A, Sopko G, Marchenko A, Ali IS, Pohost G, Sinisa Gradinac S, Abraham WT, Yii M, Prabhakaran D, Szwed H, Ferrazzi P, Petrie MC, O'Connor CM, Panchavinnin P, She L, Bonow RO, Rankin GR, Jones RH, Rouleau J-L, for the STICH Investigators. Coronary-artery bypass surgery in patients with left ventricular dysfunction. *N Engl J Med* 2011;364:1607−1616.
17. Grayburn PA, Fehske W, Omran H, Brickner ME, Lüderitz B. Multiplane transesophageal echocardiographic assessment of mitral regurgitation by Doppler color flow mapping of the vena contracta. *Am J Cardiol* 1994;74:912−917.
18. Pu M, Vandervoort PM, Griffin BP, Leung DY, Stewart WJ, Cosgrove DM III, Thomas JD. Quantification of mitral regurgitation by the proximal convergence method using transesophageal echocardiography. Clinical validation of a geometric correction for proximal flow constraint. *Circulation* 1995;92:2169−2177.
19. Pu M, Thomas JD, Vandervoort PM, Stewart WJ, Cosgrove DM, Griffin BP. Comparison of quantitative and semiquantitative methods

for assessing mitral regurgitation by transesophageal echocardiography. *Am J Cardiol* 2001;87:66−70.
20. Sugeng L, Spencer KT, Mor-Avi V, DeCara JM, Bednarz JE, Weinert L, Korcarz CE, Lammertin G, Balasia B, Jayakar D, Jeevanandam V, Lang RM. Dynamic three-dimensional color flow Doppler: an improved technique for the assessment of mitral regurgitation. *Echocardiography* 2003;20:265−273.
21. Chin JH, Lee EH, Choi DK, Choi IC. The effect of depth of anesthesia on the severity of mitral regurgitation as measured by transesophageal echocardiography. *J Cardiothorac Vasc Anesth* 2012;26:994−998.
22. Oh JK, Velazquez EJ, Menicanti L, Pohost GM, Bonow RO, Lin G, Hellkamp AS, Ferrazzi P, Wos S, Rao V, Berman D, Bochenek A, Cherniavsky A, Rogowski J, Rouleau JL, Lee KL; on behalf of the STICH Investigators. Influence of baseline left ventricular function on the clinical outcome of surgical ventricular reconstruction in patients with ischaemic cardiomyopathy. *Eur Heart J* 2013;34:39−47.
23. Zoghbi WA, Enriquez-Sarano M, Foster E, Grayburn PA, Kraft CD, Levine RA, Nihoyannopoulos P, Otto CM, Quinones MA, Rakowski H, Stewart WJ, Waggoner A, Weissman NJ. Recommendations for evaluation of the severity of native valvular regurgitation with two-dimensional and Doppler echocardiography. *J Am Soc Echocardiogr* 2003;16:777−802.
24. Lancellottti P, Moura L, Pierard L, Agricola E, Popescu BA, Tribouilloy C, Hagendorff A, Monin J-L, Badano L, Zamorano JL. European Association of Echocardiography recommendations for the assessment of valvular regurgitation. Part 2. Mitral and tricuspid regurgitation (native disease). *Eur J Echocardiogr* 2010;11:307−332.
25. Lang RM, Badano LP, Tsang W, Adams DH, Agricola E, Buck T, Faletra FF, Franke A, Hung J, Perez de Isla L, Kamp O, Kasprzak JD, Lancellotti P, Marwick TH, McCulloch ML, Monaghan MJ, Nihoyannopoulos P, Pandian NG, Pellikka PA, Pepi M, Roberson DA, Shernan SK, Shirali GS, Sugeng L, Ten Cate FJ, Vannan MA, Zamorano JL, Zoghbi WA. EAE/ASE recommendations for image acquisition and display using three-dimensional echocardiography. *J Am Soc Echocardiogr* 2012;25:3−46.
26. Grayburn PA, Weissman NJ, Zamorano JL. Quantitation of mitral regurgitation. *Circulation* 2012;126:2005−2017.